



HAL
open science

From semi-metal to superconductor: The New Mo₁₂ Cluster Sulfides Rb_{1+x}Mo₁₂S₁₄ (x = 0.08, and 1.65)

Patrick Gougeon, Philippe Gall

► **To cite this version:**

Patrick Gougeon, Philippe Gall. From semi-metal to superconductor: The New Mo₁₂ Cluster Sulfides Rb_{1+x}Mo₁₂S₁₄ (x = 0.08, and 1.65). *Journal of Alloys and Compounds*, 2021, 872, pp.159595. 10.1016/j.jallcom.2021.159595 . hal-03225466

HAL Id: hal-03225466

<https://hal.science/hal-03225466>

Submitted on 10 Jun 2021

HAL is a multi-disciplinary open access archive for the deposit and dissemination of scientific research documents, whether they are published or not. The documents may come from teaching and research institutions in France or abroad, or from public or private research centers.

L'archive ouverte pluridisciplinaire **HAL**, est destinée au dépôt et à la diffusion de documents scientifiques de niveau recherche, publiés ou non, émanant des établissements d'enseignement et de recherche français ou étrangers, des laboratoires publics ou privés.

From semi-metal to superconductor: The New Mo₁₂ Cluster Sulfides Rb_{1+x}Mo₁₂S₁₄ (x = 0.08, and 1.65)

Patrick Gougeon* and, Philippe Gall

Sciences Chimiques de Rennes, UMR 6226 CNRS – INSA – Université de Rennes 1, Avenue du Général Leclerc, 35042 Rennes, France.

*Corresponding author: patrick.gougeon@univ-rennes1.fr

Abstract

The novel Mo₁₂ cluster sulfides Rb_{2.65}Mo₁₂S₁₄ have been synthesized by direct solid-state reaction at a temperature of about 1500°C in a welded Mo tubing. The crystal structure of Rb_{2.65}Mo₁₂S₁₄ (space group P-31c: $a = 9.2828(6)$ Å, $c = 16.446(5)$ Å) was solved from X-ray single-crystal data. It is isomorphous with the K_{1+x}Mo₁₂S₁₄ compounds in which x ranges from 0 to 1.6. Consequently, the Mo-S network presents interconnected Mo₁₂S₁₄ cluster units delimiting large tunnels that are randomly occupied by a part of the Rb⁺ ions, the other ones being localized in large voids between two consecutive Mo₁₂S₁₄ units along the [001] direction. By topochemical redox reactions at around 90°C, we could remove a part of the Rb⁺ ions from the channels and thus, form the oxidized phase Rb_{1.08}Mo₁₂S₁₄. Electrical resistivity measurements performed on single crystals of Rb_{2.65}Mo₁₂S₁₄ and Rb_{1.08}Mo₁₂S₁₄ shows that the oxidized form is a semimetal while the reduced form is a metal and becomes superconducting below 4.07 K. The evolution of Mo-Mo bond lengths within the trioctahedral Mo₁₂ cluster with respect to the cationic charge x is discussed and, compared with that found in the potassium series.

Keywords: reduced molybdenum sulfide; molybdenum clusters; tunnelled structure; soft chemistry; cationic mobility; resistivity measurement; superconductor.

1. Introduction

During the last forty years, numerous reduced molybdenum sulfides, selenides, and tellurides containing metallic aggregates, often called clusters, with various sizes and forms were synthesized by solid-state reaction in the temperature range 1000-1900 °C. The octahedral Mo_6 clusters [1] is the most encountered in the Mo chalcogenide phases and lead in the latter phases to unusual electrical and magnetic properties [2-6]. Mo clusters having more than six Mo atoms such as Mo_9 [7, 8], Mo_{12} [9-11], Mo_{15} [10, 12, 13], Mo_{18} [10, 14], Mo_{21} [15, 16], Mo_{24} [10], Mo_{30} [17], and Mo_{36} [18] result from the one dimensional condensation of 2, 3, 4, 5, 6, 7, 9 and 11 octahedral clusters, respectively, through opposite faces. Most of the sulfur, selenium, and tellurium compounds based on the latter clusters have a well-defined cationic stoichiometry after being synthesized by direct solid-state syntheses in temperature range 1000°C – 1900°C. Nevertheless, the stoichiometry in cations and, consequently, the number of electrons of the Mo clusters of the latter compounds, can be modified by redox reactions made at temperature under 600°C. This leads, in particular, to a modification of some physical properties. Thus, the superconducting phases $\text{Hg}_{-4.2}\text{Mo}_{15}\text{X}_{19}$ ($\text{X} = \text{S}, \text{Se}$) [19], in which the mercury forms either Hg^{2+} or Hg_3^{2+} polycations, were obtained at 400°C by inserting mercury atoms into the metastable $\text{Mo}_{15}\text{X}_{19}$ binaries, the latter compounds being obtained after removing the indium from the semiconducting compounds $\text{In}_{-3.5}\text{Mo}_{15}\text{X}_{19}$. Likewise, in a previous paper, we described the novel compound $\text{K}_{2.3}\text{Mo}_{12}\text{S}_{14}$ [20]. Its crystal structure comprises $\text{Mo}_{12}\text{S}_{14}$ units, which delimit vast unidirectional tunnels in which some K^+ cations are delocalized. From topochemical redox reactions at 90°C, we were able to vary

the content in K^+ ions in the tunnels in order to obtain the isostructural compounds $K_{1+x}Mo_{12}S_{14}$ in which the potassium content vary between 0 and 1.6. The electrical resistivity studies realized on monocrystalline specimens of the two ternary compounds $K_{2.3}Mo_{12}S_{14}$ and $KMo_{12}S_{14}$ revealed clearly the role of the metal electron count (MEC) of the Mo_{12} cluster resulting from the cationic charge transfer toward the Mo aggregates on the electrical behavior. In particular, the former compound behaves like a semi-conductor between 300 and 4.2 K while the latter is metallic. We have continued this study by substituting potassium with rubidium. We present, here, the syntheses, crystal structures and, electrical resistivity measurements of the new compound $Rb_{2.65}Mo_{12}S_{14}$ and its oxidized form $Rb_{1.08}Mo_{12}S_{14}$. The latter was obtained by topochemical redox reactions in an aqueous solution of diiodide at low temperature. Consequently, the electrical behavior changes from a semiconductor behavior for the reduced form $Rb_{2.65}Mo_{12}S_{14}$ to a metallic behavior accompanied by a superconductive state below 4.07 K for the oxidized form that was confirmed by magnetic susceptibility measurements. The variations of the different Mo-Mo bond lengths as a function of the cationic charge will be also discussed and, compared with those found in the series $K_{1+x}Mo_{12}S_{14}$.

2. Experimental Section

2.1 Syntheses

Powders of MoS_2 , Rb_2MoS_4 and Mo were used as starting reagents. Prior to use, the molybdenum powder (purity 99.999%) was heated at 1000°C during 10 hours under a dihydrogen flowing gas for eliminating traces. The Molybdenite was synthesized from a pellet of the elements Mo and S (purity 99.999%) in stoichiometric proportion in a silica tube

sealed under dynamic vacuum, and then heated at 800° C for 48 hours. Rb_2MoS_4 was synthesized by sulfurization of Rb_2MoO_4 under a flow of CS_2 using argon as carrier gas at 400°C during 48 hours. Rb_2MoO_4 was obtained by heating an equimolar ratio of MoO_3 (99.95%) and Rb_2CO_3 (99.9%) in an alumina boat at 800°C in air during 48 hours. The purity of all the starting reagents was checked by X-ray diffraction on powder samples. In order to avoid any contamination by oxygen and humidity, the starting materials were kept and handled in a glove box under argon.

$\text{Rb}_{2.65}\text{Mo}_{12}\text{S}_{14}$ single-crystals were grown by heating at 1500 °C for 6 hours a mixture of Rb_2MoS_4 , MoS_2 and Mo having the composition $\text{Rb}_{0.091}\text{Mo}_{0.420}\text{S}_{0.489}$ in a welded Mo tubing. The heating and cooling rate were $300^\circ\text{C}\cdot\text{h}^{-1}$ and $100^\circ\text{C}\cdot\text{h}^{-1}$, respectively

The $\text{Rb}_{1.08}\text{Mo}_{12}\text{S}_{14}$ compound was obtained by an oxidation reaction of single crystals of $\text{Rb}_{2.65}\text{Mo}_{12}\text{S}_{14}$ in an aqueous solution of diiodine heated at 90°C for 48 h, in accordance with the following reaction equation: $\text{Rb}_{2.65}\text{Mo}_{12}\text{S}_{14} + 0.79 \text{I}_2 \rightarrow \text{Rb}_{1.08}\text{Mo}_{12}\text{S}_{14} + 1.57 \text{KI}$

It is interesting to note that reactions at higher temperatures or with longer reaction times did not completely empty the channels of the Rb atoms (to get $\text{RbMo}_{12}\text{S}_{14}$) as in the potassium series.

Figure 1a shows a crystal of $\text{Rb}_{2.65}\text{Mo}_{12}\text{S}_{14}$ as grown while a crystal of $\text{Rb}_{1.08}\text{Mo}_{12}\text{S}_{14}$ after Rb removal is shown in Figure 1b.

2.2 Single Crystal X-ray Studies

Black single-crystals of $\text{Rb}_{2.65}\text{Mo}_{12}\text{S}_{14}$ and $\text{Rb}_{1.08}\text{Mo}_{12}\text{S}_{14}$ were analyzed using the ω -2 θ scan technique at 20°C on an Enraf Nonius CAD-4 diffractometer equipped with a graphite-monochromator and an X-ray tube with an Mo anode ($\lambda = 0.71073 \text{ \AA}$). Unit cell parameters were determined from the refinements of the setting angles of 25 reflections at high theta

angles. For the two compounds, the orientation and intensity of 3 standard reflections were checked at interval of 250 reflections and each hour without any significant variation when recording the diffracted intensities. The collected data were subsequently corrected for Lorentz-polarization and an absorption correction was applied with the psi-scan or spherical methods implemented in the WINGX software [21]. Reflections hhl with $l = 2n+1$ being absent indicated the space groups P31c and P-31c as possible.

The positional parameters of $\text{KMo}_{12}\text{S}_{14}$ were used as starting values for the refinement of $\text{Rb}_{2.65}\text{Mo}_{12}\text{S}_{14}$ in P -31c. At this stage, the R1 factor converges to $R = 0.0544$ and, a difference Fourier map revealed an almost continuous electron density in the channel extending along the [001] direction that we modeled using five Rb atoms (Fig. 2a). The final refinement, that includes the atomic positions, anisotropic displacement parameters as well as the multiplicity factors of the Rb2, Rb3, Rb4, Rb5 and Rb6 sites with the SHELX software [22], led to the value $R1 = 0.0293$ with the 2243 independent reflections with $I/\sigma(I) > 2$ and to the maximum and minimum residual peaks of 1.55 and $-1.33 \text{ e}/\text{\AA}^3$ in the tunnel extending along the c axis (Figure 2b). Attempts to introduce anharmonic atomic displacement parameters for the Rb atoms in the channels using the program JANA2006 [23] were unsuccessful as, in our case; the diffracting centers are very distant. Indeed, the development of Gram-Charlier is applicable only for small displacement with regard to the atomic position, the limit being lower than the interatomic distances [24].

For the crystal structure of $\text{Rb}_{1.08}\text{Mo}_{12}\text{S}_{14}$, we used as starting values the atomic positional parameters of the Rb, Mo, and S atoms forming the skeleton $\text{RbMo}_{12}\text{S}_{14}$. At this stage, we observed a small electron density in the tunnel corresponding to 0.08 Rb atoms. The crystallographic and experimental data of the two studied crystals are given in Table 1, selected interatomic distances in Table 2 and, fractional atomic coordinates and equivalent isotropic displacement parameters, in table 3.

2.3 Measurements of the thermal dependence of the electrical resistivity

Electrical resistivity measurements were performed on single crystals of $\text{Rb}_{2.65}\text{Mo}_{12}\text{S}_{14}$ and $\text{Rb}_{1.08}\text{Mo}_{12}\text{S}_{14}$ using a 4-probe method and a ac current (0.1 mA) between 2 and 300 K.

The electrical contacts on the single crystals consisted of ultrasonically soldered indium. The ohmic behavior and the phase invariance were verified during the measurements.

2.4 Magnetic susceptibility measurements

Susceptibility data were collected in zero-field-cooled (ZFC) mode on a batch of randomly crystals of $\text{Rb}_{\sim 1.08}\text{Mo}_{12}\text{S}_{14}$ and $\text{Rb}_{\sim 2.65}\text{Mo}_{12}\text{S}_{14}$ using a Quantum Design SQUID magnetometer between 1.8 K and 10 K and at an applied field of 10 Oe.

3. Results and Discussion

3.1 Crystal Structure

The $\text{Rb}_x\text{Mo}_{12}\text{S}_{14}$ compounds crystallize in the structural type $\text{K}_{2.3}\text{Mo}_{12}\text{S}_{14}$ [20] in which the Mo-S network is composed of $\text{Mo}_{12}\text{S}_{14}$ clusters interconnected through Mo1-S1 interunit bonds (Figure 3). The $\text{Mo}_{12}\text{S}_{14}$ units (Figure 4) are centered on 2d positions having the C_{3i} symmetry and results from the unidirectional condensation of three Mo_6S_8 units.

As mentioned in previous publications on Mo condensed cluster sulfides and selenides, the Mo-Mo bond lengths can be classified in two categories. The first one includes

the Mo-Mo distances in the (Mo1)₃ and (Mo2)₃ triangles perpendicular to the threefold axis also called intratriangle. The latter distances are 2.6373(4) and 2.6916(8) Å in Rb_{2.65}Mo₁₂S₁₄ and Rb_{1.08}Mo₁₂S₁₄, respectively. In the K_{1+x}Mo₁₂S₁₄ (0 ≤ x ≤ 1.6) series [20], they vary between 2.638 Å and 2.686 Å with the shortest one observed in K_{2.6}Mo₁₂S₁₄ and the longest one in KMo₁₂S₁₄. The second category corresponds to the Mo-Mo distances between the Mo triangles that range from 2.6585(6) to 2.7879(6) Å in Rb_{2.65}Mo₁₂S₁₄ and from 2.6458(10) to 2.8423(8) Å in Rb_{1.08}Mo₁₂S₁₄ compared to 2.634 Å to 2.841 Å in the K_{1+x}Mo₁₂S₁₄ (0 ≤ x ≤ 1.6) series. In 1983, extended Hückel calculations performed by Hughbanks and Hoffmann [25] showed that the number of electrons per Mo₁₂ cluster could vary between 44 and 50, the latter value corresponding to the close-shell configuration. The previous study, we made on the compounds K_{1+x}Mo₁₂S₁₄ (0 ≤ x ≤ 1.6) with a MEC varying between 45 and 46.6 per Mo₁₂ cluster, has revealed that the Mo-Mo bond lengths are strongly correlated to the variation of the cationic charge transfer towards the Mo₁₂ clusters. Thus, the increase of the MEC of the Mo₁₂ aggregate when we passed from the compound KMo₁₂S₁₄ with 45e⁻/Mo₁₂ to the compound K_{2.6}Mo₁₂S₁₄ having 46.6 e⁻/Mo₁₂ leads, excluding the inter-triangle Mo2-Mo2 bond lengths that moderately increases and thus present an anti-binding character, in a shortening of the remaining distances between the Mo atoms of the cluster (see circles in figure 5) that reflects their binding character. The mean distances between the Mo atoms in the Mo₁₂ cluster diminish as the number of electrons per cluster increase as represented in Figure 6. As we can see in figure 5 and 6, the Mo-Mo distances observed in the new two Rb compounds (see squares in figure 5) fit well with those found in the K_{1+x}Mo₁₂S₁₄ (0 ≤ x ≤ 1.6) series and, consequently, an overall contraction of the trioctahedral Mo₁₂ cluster is also observed with a distance between the two ending Mo₃ triangles of 6.74 Å in Rb_{2.65}Mo₁₂S₁₄ and 6.81 Å in Rb_{1.08}Mo₁₂S₁₄.

The Mo-S bond lengths are similar those previously observed in other reduced molybdenum sulfides. The shortest Mo-S distances (c.a. 2.38 Å) are observed for the S3 atoms capping the ending Mo₃ triangle formed by the Mo1 atoms. The longest Mo-S distances (c.a. 2.60 Å) involve the internal S2 atoms and, also the Mo1 atoms of the ending Mo₃ triangles. Each Mo₁₂S₁₄ group is linked to 6 adjacent ones through twelve Mo1-S1 bonds, called interunit, ranging from 2.434 to 2.484 Å. The whole forms the three-dimensional Mo-S network with the shortest Mo-Mo intercluster distance being 3.3262(3) Å in Rb_{2.65}Mo₁₂S₁₄ and 3.1645(8) Å in Rb_{1.08}Mo₁₂S₁₄ compared to 3.263 Å and 3.135 Å and in K_{2.6}Mo₁₂S₁₄ and KMo₁₂S₁₄.

As revealed by the Figure 7 showing the structure of Rb_{2.65}Mo₁₂S₁₄ viewed down the [001] direction, it results from this arrangement that large tunnels running in the c axis are generated in which the Rb2, Rb3, Rb4, Rb5 and Rb6 atoms of Rb_{2.65}Mo₁₂S₁₄ are observed. The remaining rubidium atoms (i.e. Rb1) occupy voids delimited by the Mo₁₂S₁₄ units. Eight sulfur atoms surround the Rb1 atoms. Six of them (S2) form a flattened octahedron in the c direction and, the other two S3 atoms each cap the opposite triangular faces of the sulfur octahedron (Figure 8). Figure 9 shows the environments of the rubidium cations located in the channels of the crystal of Rb_{2.65}Mo₁₂S₁₄. The Rb3 and Rb5 atoms are each surrounded by 6 sulphur atoms forming a trigonal antiprism with Rb-S contacts comprise between 3.31 (3) and 3.4410(7) Å. The Rb2, Rb4, and Rb6 atoms occupy distorted tricapped trigonal prisms of S atoms with Rb distances spreading in a large range 3.106(15) – 4.01(8) Å. By using the bond valence sum (BVS) for Rb-S bonds [26], we found an average oxidation state of +1.08 for the rubidium, slightly larger than expected, that perhaps reflects the high thermal motions and partial occupancy factors of the Rb atoms, which tend to make the observed bond lengths shorter and the BVS larger.

3.2 Resistivity and Magnetic Measurements

The temperature dependencies of the electrical resistivities measured on single crystals of $\text{Rb}_{2.65}\text{Mo}_{12}\text{S}_{14}$ and $\text{Rb}_{\sim 1.08}\text{Mo}_{12}\text{S}_{14}$ in the 2-290 K temperature range are presented in Figure 10. $\text{Rb}_{\sim 1.08}\text{Mo}_{12}\text{S}_{14}$ behaves like a metal with a resistivity of $0.6 \mu\Omega\cdot\text{cm}$ at 300 K and becomes superconducting below 4.07 K (middle transition at 3.8 K). In the case of $\text{Rb}_{\sim 2.65}\text{Mo}_{12}\text{S}_{14}$, the temperature variation of the resistivity indicates a semi-metal behavior with a resistivity of $1.1 \mu\Omega\cdot\text{cm}$ at the ambient temperature. Superconductivity (T_c onset at 3.9 K) was confirmed from magnetic susceptibility measurements in ZFC mode on a batch of randomly oriented crystals of $\text{Rb}_{\sim 1.08}\text{Mo}_{12}\text{S}_{14}$ while for $\text{Rb}_{2.65}\text{Mo}_{12}\text{S}_{14}$, no Meissner effect was observed down to 1.8 K (Figure 11). This change in behavior comes mainly from the MEC that increases from $45.08 e^-$ by cluster Mo_{12} in $\text{Rb}_{\sim 1.08}\text{Mo}_{12}\text{S}_{14}$ to $46.65 e^-/\text{Mo}_{12}$ in $\text{Rb}_{\sim 2.65}\text{Mo}_{12}\text{S}_{14}$ and was also previously observed for the $\text{KMo}_{12}\text{S}_{14}$ and $\text{K}_{2.6}\text{Mo}_{12}\text{S}_{14}$ compounds with 45 and $46.6 e^-/\text{Mo}_{12}$, respectively. Such modification of the physical properties with respect to the number of electrons per Mo cluster has also been observed for the selenide $\text{Ag}_{3.6}\text{Mo}_9\text{Se}_{11}$ [7] containing bioctahedral Mo_9 clusters with $35.6 e^-$ and synthesized by solid-state chemistry which presents a semiconducting behavior while the metastable $o\text{-Mo}_9\text{Se}_{11}$ binary compound [27], resulting from the removal of the silver atoms at 80°C and having $32 e^-$ per Mo_9 clusters, is metallic, and also presents a superconducting state under 5.5 K. In contrast, the superconductivity observed under 4.4 K in the Mo_{12} cluster compound $\text{Cs}_2\text{Mo}_{12}\text{Se}_{14}$ ($46 e^-/\text{Mo}_{12}$) is quickly destroyed by the insertion of Cu in the series of compounds $\text{Cu}_x\text{Cs}_2\text{Mo}_{12}\text{Se}_{14}$ ($0 \leq x \leq 2$) [28].

4. Conclusion

The new two compounds $\text{Rb}_{2.65}\text{Mo}_{12}\text{S}_{14}$ and $\text{Rb}_{1.08}\text{Mo}_{12}\text{S}_{14}$ were prepared by direct solid-state synthesis at 1500°C and by soft chemistry at 90°C , respectively. Single-crystal X-ray diffraction studies showed that their crystal structures contain quasi-isolated $\text{Mo}_{12}\text{S}_{14}$ units forming a three-dimensional network characterized by channels extending along the c axis in which a part of the rubidium cations are delocalized. The decrease of the cationic charge transfer towards the Mo_{12} cluster leads to an increase of the mean Mo-Mo bond-lengths in the Mo_{12} aggregate, and to a variation of the electrical since we go from a semi-conducting behavior for $\text{Rb}_{2.65}\text{Mo}_{12}\text{S}_{14}$ to a metallic one for the oxidized $\text{Rb}_{1.08}\text{Mo}_{12}\text{S}_{14}$ compound that also becomes superconductor below 4.07 K . More investigations on the superconducting properties as well as thermoelectrical studies for the reduced form will be the subjects of further works on these compounds. On the other hand, due the large tunnels extending along the c axis, the molybdenum-sulfur framework of the $\text{Rb}_x\text{Mo}_{12}\text{S}_{14}$ compounds is especially well appropriate for topochemical reactions by soft chemistry or electrochemistry, leading to the design of novel superconductors. Therefore, it will be interesting to replace the rubidium atoms present in the channels with other cations such as lead, thallium or mercury. In particular, several studies have demonstrated that Tl-containing cluster compounds may display very low thermal conductivities (K) [29-31] that is one of the important factors for having interesting thermoelectric properties. This has been confirmed by recent investigations of the thermoelectric properties of the $\text{Ag}_x\text{Mo}_9\text{Se}_{11}$ ($3.4 \leq x \leq 3.9$) [32] and $\text{Ag}_2\text{Tl}_2\text{Mo}_9\text{Se}_{11}$ [33] compounds that reveal very low K values leading to interesting ZT values at high temperatures with a maximum of 0.65 at 550°C . On the other hand, mercury should also lead to a superconducting state at low temperatures since, until now, the insertion of mercury in the compounds with condensed clusters systematically led to the appearance of

superconductivity as observed in the $\text{Hg}_{-4.2}\text{Mo}_{15}\text{X}_{19}$ ($\text{X} = \text{S}, \text{Se}$) [34] and $\text{Hg}_{-2.8}\text{KMo}_{12}\text{S}_{14}$ [35].

References

- [1] R. Chevrel, M. Sergent, J. Prigent, *J. Solid State Chem.* 3 (1971) 515.
- [2] Ø. Fischer, *Appl. Phys.* 16 (1978) 1.
- [3] O. Pena, M. Sergent, *Prog. Solid State Chem.* 19 (1989) 165.
- [4] D. H. Douglass (ed.), in *Superconductivity in d- and f-band Metals* (Plenum Press, New York, 1986).
- [5] G. K. Shenoy, B. D. Dunlap, F. Y. Fradin (eds.), *Ternary Superconductors* (North Holland, New York, Amsterdam, Oxford, 1981).
- [6] Ø. Fischer and M. B. Maple (eds.), *Topics in Current Physics*, vol. 32/34: Superconductivity in Ternary Compounds, Tomes I and II. (Springer, Berlin, Heidelberg, New York, 1982).
- [7] P. Gougeon, J. Padiou, J. Y. Le Marouille, M. Potel, M. Sergent, *J. Solid State Chem.* **51** (1984) 218.
- [8] S. Picard, J.-F. Halet, P. Gougeon, M. Potel, *Inorg. Chem.* 38 (1999) 4422.
- [9] P. Gougeon, M. Potel, J. Padiou, M. Sergent, *Mat. Res. Bull.* **22** (1988) 1087.
- [10] C. Thomas, S. Picard, R. Gautier, P. Gougeon, M. Potel, *J. Alloys Comp.* 262-263 (1997) 305.
- [11] R. Gautier, S. Picard, P. Gougeon, M. Potel, *Mat. Res. Bull.* 34 (1999) 93-101.
- [12] P. Gougeon, M. Potel, M. Sergent, *Acta Cryst.* **C45** (1989) 182.
- [13] P. Gougeon, M. Potel, M. Sergent, *Acta Cryst.* **C45** (1989) 1413.
- [14] P. Gougeon, M. Potel, J. Padiou, M. Sergent, *Mat. Res. Bull.* **23** (1988) 453.
- [15] P. Gougeon, M. Potel, M. Sergent, *Acta Cryst.* **C46** (1990) 2284.

- [16] S. Picard P. Gougeon, M. Potel, *Acta Cryst.* **C53** (1997) 1519.
- [17] P. Gougeon
- [18] S. Picard, M. Potel, P. Gougeon, *Angew. Chem.* **38** (1999) 2023.
- [19] D. Salloum, P. Gougeon M. Potel, R. Gautier, *Comptes Rendus Chimie*, 8(11-12) (2005) 1743-1749
- [20] S. Picard, P. Gougeon, M. Potel, *Inorg. Chem.* 45 (2006) 1611.
- [21] L. J. Farrugia, *J. Appl. Crystallogr.*, 1999, 32, 837-838.
- [22] G. M. Sheldrick, *SHELXL97*, Program for the Refinement of Crystal Structures, University of Göttingen, Germany, 1997.
- [23] V. Petricek, M. Dusek and L. Palatinus, *JANA2006* Crystallographic computing system, 2006.
- [24] W. F. Kuhs, *Acta Cryst.* A48 (1992) 80-98.
- [25] Hughbanks, T.; Hoffmann, R. *J. Am. Chem. Soc.* **1983**, 105, 1150.
- [26] I.D. Brown, *Chem. Rev.*, 109 (2009) 6858-6919.
- [27] P. Gougeon, M. Potel, J. Padiou, M. Sergent, C. Boulanger, J.M. Lecuire, *Journal of Solid State Chemistry*, 71(2) (1987) 543-551.
- [28] R.A.R. Al Orabi, B. Fontaine, R. Gautier, P. Gougeon, P. Gall, Y. Bouyrie, A. Dauscher, C. Candolfi, B. Lenoir, *Inorganic Chemistry*, 55(13) (2016) 6616-6624.
- [29] S. Yamanaka, K. Kurosaki, A. Kosuga, K. Goto, H. Muta, *MRS Symp. Proc.*, 886 (2006) 337-341.
- [30] K. Kurosaki, A. Kosuga, H. Muta, M. Uno, S. Yamanaka, *Appl. Phys. Lett.*, 87 (2005) 061919.
- [31] B. Wolfing, C. Kloc, J. Teubner, E. Bucher, *Phys. Rev. Lett.*, 86 (2001) 4350-4353.
- [32] P. Gougeon, P. Gall, R.A.R. Al Orabi, B. Fontaine, R. Gautier, M. Potel, T. Zhou, B. Lenoir, M. Colin, C. Candolfi, A. Dauscher, *Chemistry of Materials* 24(15) (2012) 2899-

2908.

[33] R.A.R. Al Orabi, P. Gougeon, P. Gall, B. Fontaine, R. Gautier, M. Colin, C. Candolfi, A. Dauscher, J. Hejtmanek, B. Malaman, B. Lenoir, *Inorganic Chemistry* 53(21) (2014) 11699-11709.

[34] D. Salloum, P. Gougeon, M. Potel, R. Gautier, *Comptes Rendus Chimie* 8(11-12) (2005) 1743-1749.

[35] P. Gougeon, P. Gall, *Inorganic Chemistry* 56(6) (2017) 3440-3446.

Table 1. X-ray Crystallographic and Experimental Data for $\text{Rb}_{2.65}\text{Mo}_{12}\text{S}_{14}$ and, $\text{Rb}_{1.08}\text{Mo}_{12}\text{S}_{14}$.

Empirical formula	$\text{Rb}_{2.65}\text{Mo}_{12}\text{S}_{14}$	$\text{Rb}_{1.07}\text{Mo}_{12}\text{S}_{14}$
Formula weight	1826.62	1691.57
Temperature	293(2) K	293(2) K
Wavelength	0.71073 Å	0.71073
Crystal system, space group	Trigonal, P -31c	Trigonal, P -31c
Unit cell dimensions	a = 9.2828(6) Å c = 16.446(5) Å	a = 9.1080(6) Å c = 16.490(5) Å
Volume	1227.3(4) Å ³	1184.7(4)
Z, Calculated density	2, 4.943 Mg/m ³	2, 4.742 Mg/m ³
Absorption coefficient	12.306 mm ⁻¹	9.521 mm ⁻¹
F(000)	1652	1535
Crystal size	0.05x0.05x0.05 mm	0.14x0.14x0.10 mm
Theta range for data collection	2.477 to 44.928 deg.	2.470 to 34.827 deg.
Limiting indices	-18<=h<=0, 0<=k<=18, 0<=l<=32	0<=h<=7, 0<=k<=12, -26<=l<=26
Reflections collected/unique	7073/3386 [R(int) = 0.0376]	1996 / 1737 [R(int) = 0.0264]
Refinement method	Full-matrix least-squares on F ²	Full-matrix least-squares on F ²
Data / restraints / parameters	3386 / 0 / 62	1737 / 0 / 46
Goodness-of-fit on F ²	1.014	0.971
Final R indices [I>2σ(I)]	R1 = 0.0293, wR2 = 0.0474	R1 = 0.0390, wR2 = 0.0834
R indices (all data)	R1 = 0.0685, wR2 = 0.0531	R1 = 0.0752, wR2 = 0.0935
Extinction coefficient	0.00107(5)	0.00061(10)
Largest diff. peak and hole	1.547 and -1.329 e.Å ⁻³	1.712 and -1.624 e.Å ⁻³

Table 2. Selected interatomic bond lengths (Å) for $\text{Rb}_{2.65}\text{Mo}_{12}\text{S}_{14}$ and, $\text{Rb}_{1.08}\text{Mo}_{12}\text{S}_{14}$.

	$\text{Rb}_{2.65}\text{Mo}_{12}\text{S}_{14}$	$\text{Rb}_{1.08}\text{Mo}_{12}\text{S}_{14}$
intratriangle		
Mo1-Mo1 (x2)	2.6373(4)	2.6916(8)
Mo2-Mo2 (x2)	2.6790(4)	2.6928(8)
intertriangle		
Mo1-Mo2	2.7176(6)	2.7560(8)
	2.7879(6)	2.8423(8)
Mo2-Mo2	2.6585(6)	2.6458(10)
	2.6803(6)	2.6761(10)
intercluster		
Mo1-Mo1	3.3262(3)	3.1645(8)
Mo1-S3	2.3778(8)	2.3813(17)
Mo1-S1	2.4597(6)	2.4444(14)
	2.4809(6)	2.44468(14)
Mo1-S1	2.5003(7)	2.4587(15)
Mo1-S2 (x2)	2.5974(8)	2.6104(14)
Mo2-S1	2.4578(8)	2.4301(14)
Mo2-S2	2.4692(6)	2.4598(15)
	2.4776(7)	2.4677(15)
Mo2-S2 (x2)	2.5850(8)	2.5640(14)
Rb1-S2 (x6)	3.3974(7)	3.3117(15)
Rb1-S3 (x2)	3.024(1)	3.034(2)
Rb2-S1 (x3)	3.13(2)	
Rb2-S2 (x3)	3.58(6)	
Rb2-S1 (x3)	3.91(8)	
Rb3/Rb2-S2 (x6)	3.4410(7)	3.3662(15)
Rb4-S1 (x3)	3.106(15)	
Rb4-S1 (x3)	3.45(6)	
Rb4-S2 (x3)	4.01(8)	
Rb5-S2 (x3)	3.35(2)	
Rb5-S1 (x3)	3.31(3)	

Rb6-S2 (x3)	3.26(3)
Rb6-S2 (x3)	3.78(15)
Rb6-S1 (x3)	3.89(18)

Table 3. Fractional atomic coordinates, equivalent isotropic displacement parameters U_{eq} (\AA^2), Wyckoff positions and, site occupancy factors (s.o.f.) for $\text{Rb}_{2.65}\text{Mo}_{12}\text{S}_{14}$ and, $\text{Rb}_{1.08}\text{Mo}_{12}\text{S}_{14}$. U_{eq} is defined as one third of the trace of the orthogonalized U_{ij} tensor.

$\text{Rb}_{2.65}\text{Mo}_{12}\text{S}_{14}$

Atom	x	y	z	U_{eq}	Wyck.	s.o.f.
Mo1	0.65635(2)	0.49196(2)	0.04492(2)	0.00825(4)	12i	1
Mo2	0.49937(2)	0.33198(2)	0.18385(2)	0.00697(3)	12i	1
S1	0.35036(7)	0.31161(7)	0.05699(3)	0.01031(9)	12i	1
S2	0.36119(7)	0.02440(7)	0.18049(3)	0.01123(9)	12i	1
S3	0.6667	0.3333	0.56613(6)	0.01242(16)	4f	1
Rb1	0.6667	0.3333	0.7500	0.01921(12)	2c	1
Rb2	0.0000	0.0000	0.088(8)	0.05(4)	4e	0.008(17)
Rb3	0.0000	0.0000	0.2500	0.109(19)	2a	0.26(7)
Rb4	0.0000	0.0000	0.037(9)	0.14(7)	4e	0.16(5)
Rb5	0.0000	0.0000	0.129(6)	0.20(4)	4e	0.46(7)
Rb6	0.0000	0.0000	0.201(18)	0.20(14)	4e	0.07(6)

$\text{Rb}_{1.08}\text{Mo}_{12}\text{S}_{14}$

Atom	x	y	z	U_{eq}	Wyck.	s.o.f.
Mo1	0.50307(6)	0.34661(6)	0.04338(2)	0.00895(11)	12i	1
Mo2	0.49503(6)	0.16359(6)	0.18452(2)	0.00897(11)	12i	1
S1	0.34604(17)	0.03837(17)	0.05861(7)	0.0105(2)	12i	1
S2	0.35708(18)	0.33772(19)	0.18096(7)	0.0126(2)	12i	1
S3	0.6667	0.3333	-0.06604(13)	0.0125(4)	4f	1
Rb1	0.3333	0.6667	0.2500	0.0171(3)	2c	1
Rb2	0.0000	0.0000	0.2500	0.09(2)	2a	0.073(8)

Figure Captions

Figure 1. Photos of a crystal of $\text{Rb}_{2.65}\text{Mo}_{12}\text{S}_{14}$ (a) before and (b) after the treatment in a solution of diode (48h at 90°C).

Figure 2. Fo-Fc maps along the [001] direction in $\text{Rb}_{2.65}\text{Mo}_{12}\text{S}_{14}$ a) after refinement of the Mo-S framework (step: $1.5 \text{ e } \text{\AA}^{-3}$) and b) after the final refinement.

Figure 3. View of the crystal structure of $\text{Rb}_{2.65}\text{Mo}_{12}\text{S}_{14}$ along the [110] direction (90% probability ellipsoids).

Figure 4. View of the $\text{Mo}_{12}\text{S}_{14}\text{S}_6$ unit with its numbering scheme.

Figure 5. Variations of the different Mo-Mo bond lengths in the Mo_{12} aggregate with the overall cationic charge. Red: intertriangle Mo1-Mo2, magenta: intertriangle Mo1-Mo2, green: intratriangle Mo2-Mo2, yellow: intratriangle Mo1-Mo1, blue: intertriangle Mo2-Mo2, black: intertriangle Mo2-Mo2

Figure 6. Evolution of the mean Mo-Mo bond lengths in the Mo_{12} aggregate with the overall cationic charge.

Figure 7. View of the $\text{Rb}_{2.65}\text{Mo}_{12}\text{S}_{14}$ along the [001] direction.

Figure 8. Sulfur environment of the Rb1 cation.

Figure 9. Sulfur environments of the Rb cations located in the channels of $\text{Rb}_{2.65}\text{Mo}_{12}\text{S}_{14}$.

Figure 10 Thermal variation of the electrical resistivities of $\text{Rb}_{\sim 1.08}\text{Mo}_{12}\text{S}_{14}$ and $\text{Rb}_{\sim 2.65}\text{Mo}_{12}\text{S}_{14}$ single crystals.

Figure 11 The zero-field cooled (ZFC) temperature-dependent magnetic susceptibility of $\text{Rb}_{\sim 1.08}\text{Mo}_{12}\text{S}_{14}$ and $\text{Rb}_{\sim 2.65}\text{Mo}_{12}\text{S}_{14}$ under an applied field of 10 Oe.



Figure 1

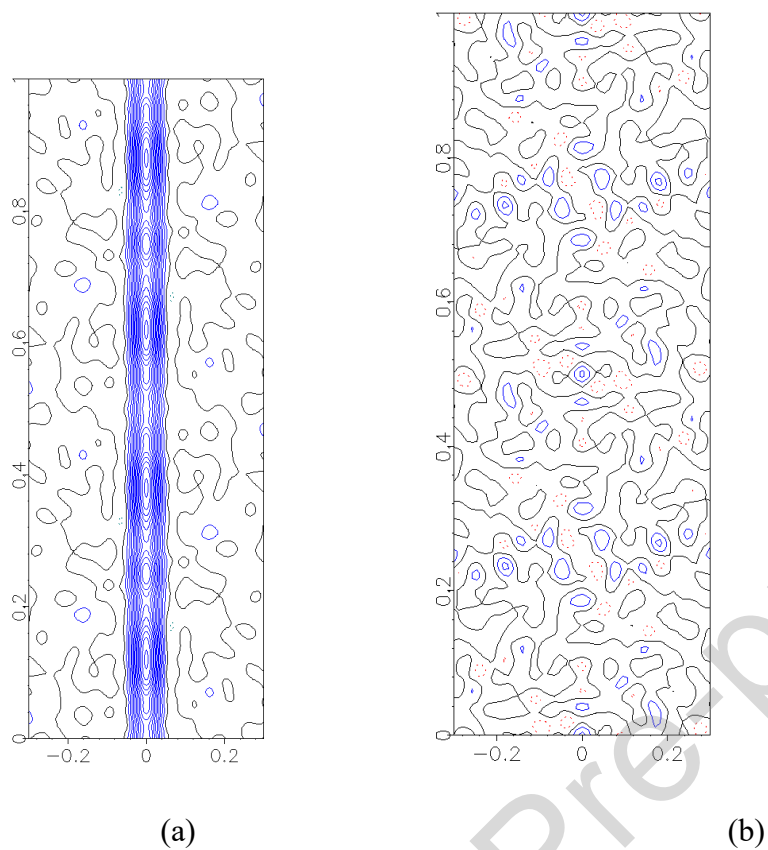


Figure 2

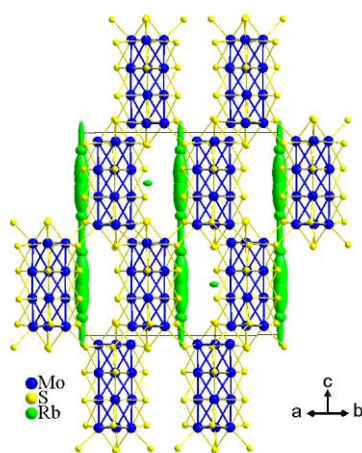


Figure 3

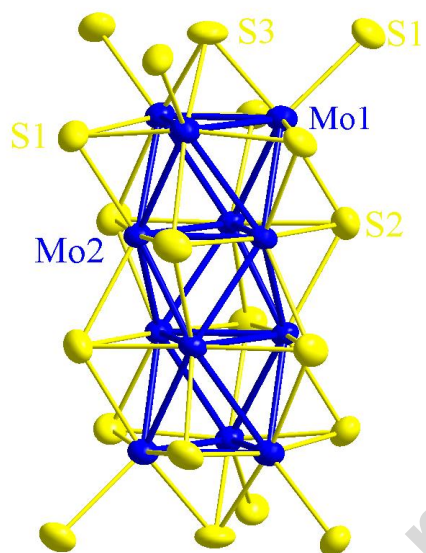


Figure 4

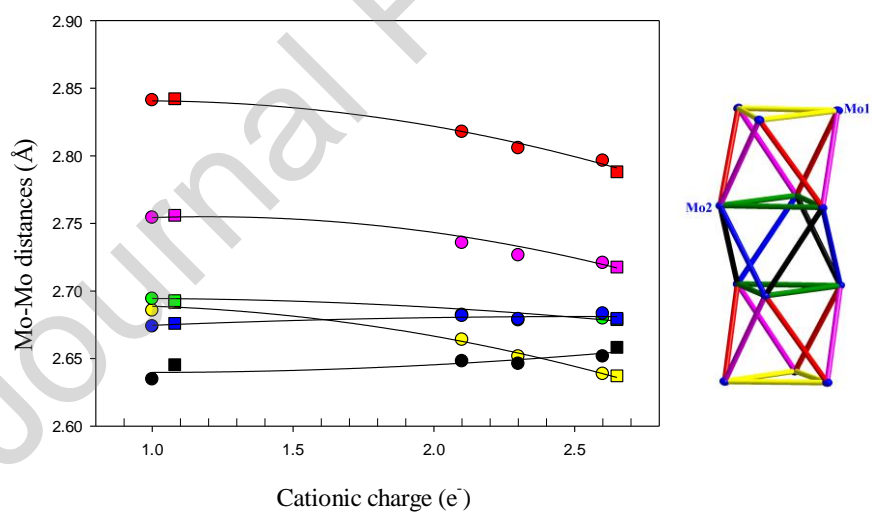


Figure 5

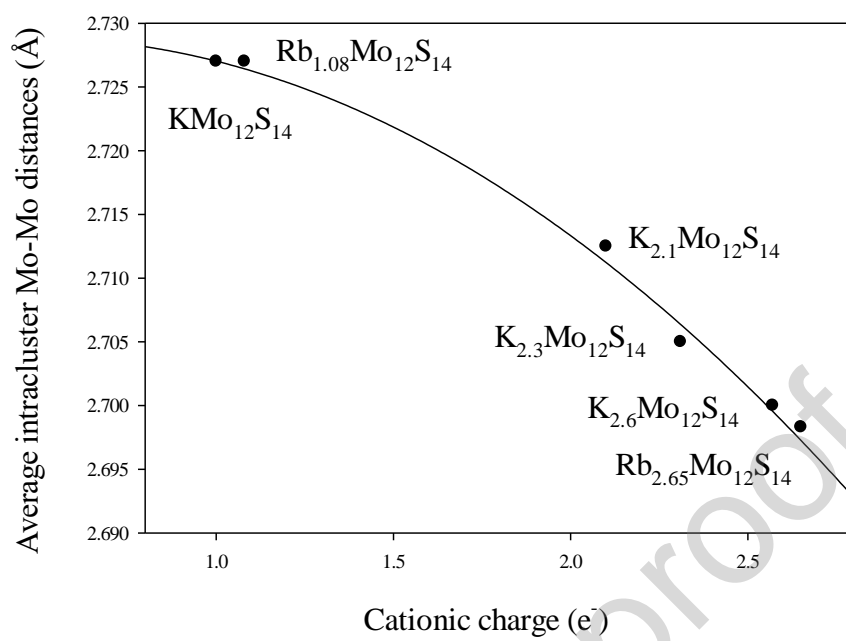


Figure 6

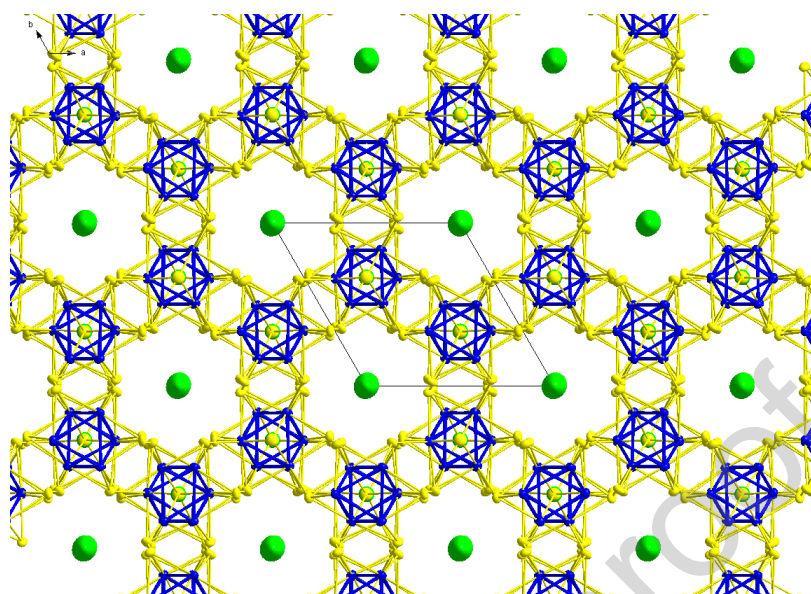


Figure 7

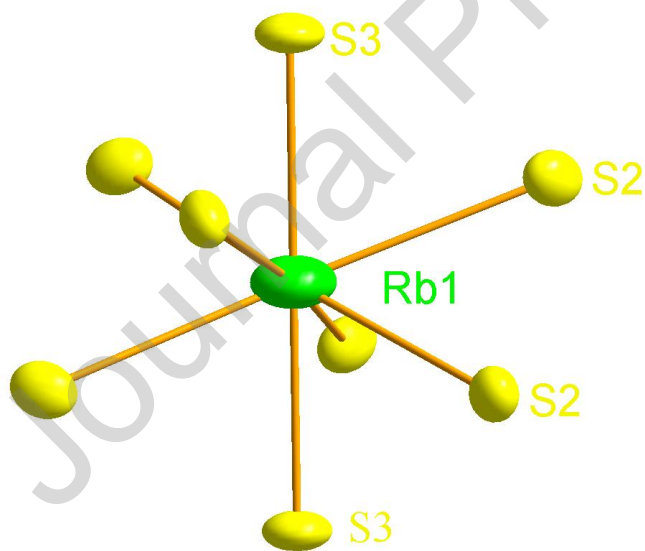


Figure 8

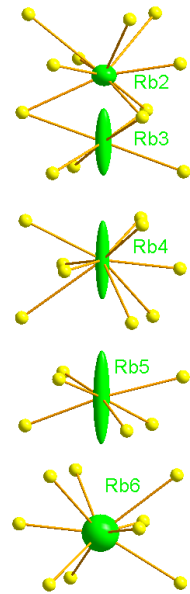


Figure 9

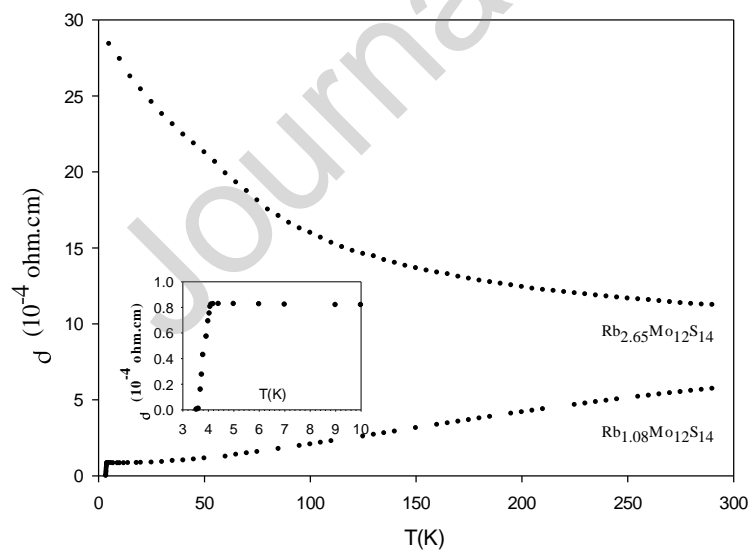


Figure 10

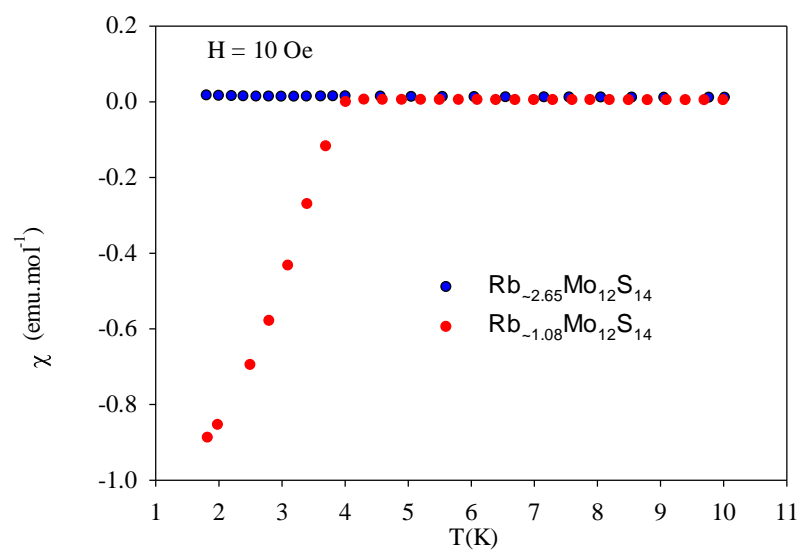
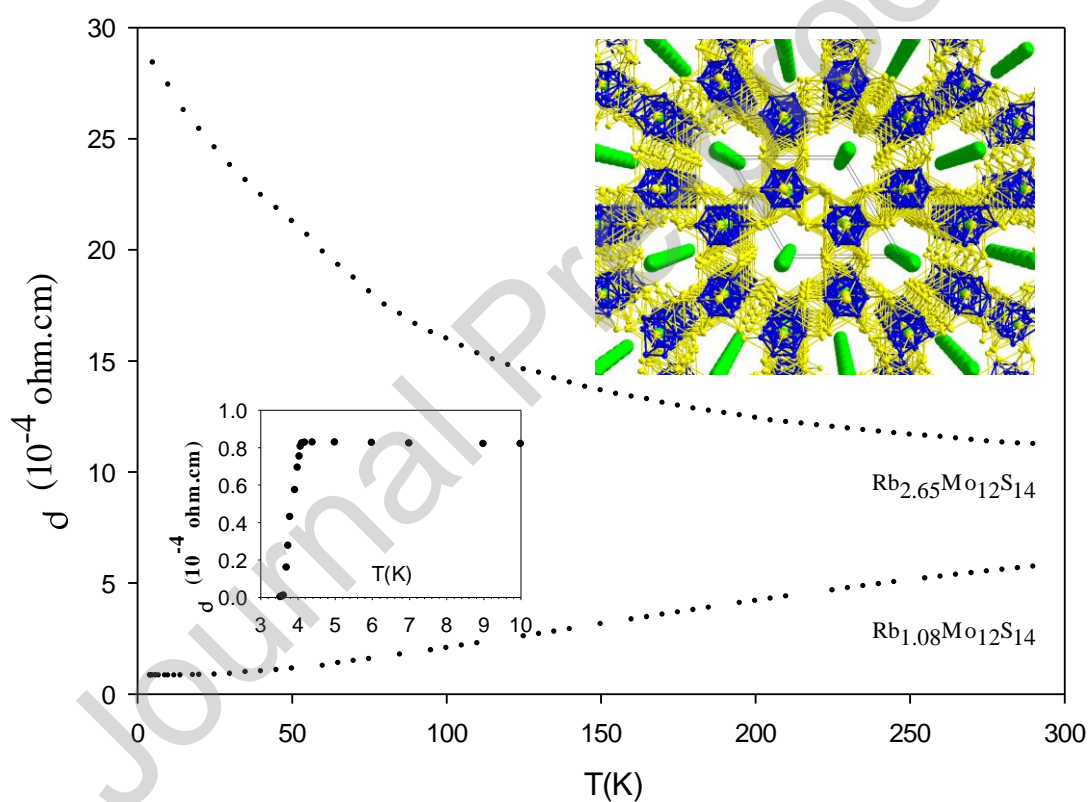


Figure 11

Graphical abstract

The crystal structures of the cluster compounds $\text{Rb}_{2.65}\text{Mo}_{12}\text{S}_{14}$ and $\text{Rb}_{1.08}\text{Mo}_{12}\text{S}_{14}$ contain tri-octahedral Mo_{12} forming $\text{Mo}_{12}\text{S}_{12}^{i}\text{S}_6^a$ units delimited large channels filled partially by Rb^+ cations. Electrical resistivity measurements carried out on single crystals of $\text{Rb}_{2.65}\text{Mo}_{12}\text{S}_{14}$ and $\text{Rb}_{1.08}\text{Mo}_{12}\text{S}_{14}$ indicate that the former is semiconducting whereas the latter is metallic with a superconducting state below 4.07 K.



CRedit authorship contribution statement

Patrick Gougeon: Structural studies, crystal growth.

Philippe Gall: Powder syntheses, physical measurements

Declaration of interests

The authors declare that they have no known competing financial interests or personal relationships that could have appeared to influence the work reported in this paper.

The authors declare the following financial interests/personal relationships which may be considered as potential competing interests:

Highlights

- Large one-dimensional channel crystal structure
- $\text{Rb}_x\text{Mo}_{12}\text{S}_{14}$ compounds are particularly well adapted for topotactic reactions by soft chemistry or electrochemistry
- Evolution of the electrical resistivity with the Rb stoichiometry
- Superconductor

Journal Pre-proof